Computers and Mathematics with Applications 65 (2013) 882–890

Contents lists available at SciVerse ScienceDirect

Computers and Mathematics with Applications

journal homepage: www.elsevier.com/locate/camwa

A comparison study of multi-component Lattice Boltzmann models for flow in porous media applications

Jianhui Yang, Edo S. Boek*

Qatar Carbonates and Carbon Storage Research Centre (QCCSRC), Department of Chemical Engineering, Imperial College London, London, SW7 2AZ, United Kingdom

ARTICLE INFO

Keywords:
Lattice Boltzmann
Multi-component models
Binary fluids

ABSTRACT

A comparison study of three different multi-component Lattice Boltzmann models is carried out to explore their capability of describing binary immiscible fluid systems. The Shan–Chen pseudo potential model, the Oxford free energy model and the colour gradient model are investigated using the multi-relaxation time scheme (MRT) algorithm to study the flow of binary immiscible fluids. We investigate Poiseuille flow of layered immiscible binary fluids and capillary fingering phenomena and evaluate the results against analytical solutions. In addition, we examine the capability of the various models to simulate fluids with significant viscosity and density contrast and suitable interface thickness. This is of great importance for large scale flow in porous media applications, where it is important to minimise the interfacial thickness from a computational point of view. We find that the Shan–Chen model can simulate high density ratios up to 800 for binary fluids with the same viscosity. Imposing a viscosity contrast will lead to highly diffusive interfaces in the Shan–Chen model and therefore this will affect significantly the numerical stability. The Free Energy model and the colour gradient model have similar capabilities on this point: they can simulate binary fluids having the same density but with significant viscosity contrast. This is of great importance to study the flow of water, supercritical CO_2 and oil in porous media, for CO_2 storage and Enhanced Oil Recovery (EOR) operations.

1. Introduction

1.1. Background

Multi-component flows are of great importance in many engineering applications, including petroleum, biochemical and chemical engineering. Several conventional CFD techniques, including the volume of fluid (VOF) and level-set methods, have been used to study multi-component flow. Interfacial dynamics at large scales can be captured by these techniques, but information of small scale interfaces is often missing [1]. The lattice-Boltzmann method (LBM) is an alternative solution for simulations of complex flow due to its statistical physics background, easy implementation, strength of dealing with complex geometries and inherent parallelism [2]. Here we will consider lattice-Boltzmann simulations to study the flow of water, supercritical CO_2 and oil in porous media, for CO_2 storage and Enhanced Oil Recovery (EOR) operations.

1.2. Multi-component lattice Boltzmann models

The lattice-Boltzmann multi-component model [3,4] was first introduced by Gunstensen et al. [5] under the name colour gradient model. Two components represent two types of fluid with their own distribution functions, and follow their own

* Corresponding author.
E-mail addresses: jianhui.yang10@imperial.ac.uk (J. Yang), e.boek@imperial.ac.uk, esb30@cam.ac.uk (E.S. Boek).

0898-1221/$ – see front matter © 2012 Elsevier Ltd. All rights reserved.
doi:10.1016/j.camwa.2012.11.022

evolution equation. They are named as red and blue particles respectively. The collision step includes self- and cross-interactions with other types of particles. A colour gradient function is introduced to calculate the surface tension between the different phases [6]. To achieve the phase separation, mixing near the interface should be minimised. A procedure called recolouring has been proposed for this minimisation process [7,8].

The free energy model was developed by Swift et al. [9]. This model includes thermodynamic equilibrium functions of phases and a term describing the surface tension is added to the equilibrium distribution function. This allows the free energy model to specify the surface tension more easily than the other multi-phase multi-component models. Also it is a fully thermodynamically consistent binary fluid lattice Boltzmann model. To reduce spurious currents, Pooley et al. [10] proposed a modified distribution function for the free energy model, decreasing spurious velocities by an order of magnitude compared to previous models.

A pseudo potential lattice-Boltzmann model was developed by Shan and Chen [11,12]. The principal characteristic of this model is an interaction force between the particles, which is introduced to have a consistent treatment of the equation of state for a non-ideal gas. Shan [13] reported that spurious velocities are due to the lack of sufficient isotropy in the calculation of the gradient term for the interaction force. Finite difference gradient operators with higher order of isotropy were proposed and spurious currents were found to decrease significantly [13–15].

2. Comparison of multi-component lattice Boltzmann models

We briefly review multi-component lattice-Boltzmann models including the Shan–Chen pseudo potential model, the free energy model and the colour gradient model. We only implement the standard multi-component LB models in this paper to investigate several fundamental issues that are of interest for flow in porous media applications.

2.1. The Shan–Chen pseudo potential model

We start with the standard LBM using the Bhatnagar–Gross–Krook (BGK) collision term. In the lattice Boltzmann method (LBM), fictional particle groups on lattice nodes with discrete velocities are used to describe fluids. A distribution function $f_i(\mathbf{x}) = f(\mathbf{x}, \mathbf{e}_i)$ is used to describe the occupation of each lattice site. Each lattice velocity $\mathbf{e}_i$ on each lattice node $\mathbf{x}$ has a distribution function $f_i(\mathbf{x})$.

Discretisation of space, velocity and time are carried out in LBM. This procedure greatly simplifies the original Boltzmann equation. The location of particles in space is restrained on the nodes of a lattice grid, and the particle velocity is simplified into a very limited number of lattice velocities. We take a 2-D model as an example. This model is well known and widely used in the application. It is two-dimensional, contains 9 velocities and has been proposed by Qian et al. [16] under the name D2Q9. In LBM, we assume all the particles have the same uniform mass (normally 1 mass unit is taken for simplicity). The lattice unit (l.u.) and the time step (ts) are important length and time units in LBM. We only discuss the uniform mesh in this chapter ($\Delta x = \Delta y$). The macroscopic hydrodynamic quantities are calculated as:

$$\rho(\mathbf{x}, t) = \sum_i f_i(\mathbf{x}, t), \tag{1}$$

$$\rho\mathbf{u}(\mathbf{x}, t) = \sum_i \mathbf{e}_i f_i(\mathbf{x}, t). \tag{2}$$

Here we use the D2Q9 lattice model [16] with nine velocities on a uniform square 2D lattice. This model is widely used in 2D LB simulations. The lattice velocity is written as:

$$\mathbf{e} = e\begin{bmatrix} 0 & 1 & 0 & -1 & 0 & 1 & -1 & -1 & 1 \\ 0 & 0 & 1 & 0 & -1 & 1 & 1 & -1 & -1 \end{bmatrix}, \tag{3}$$

where $e = \Delta x/\Delta t$ is the local lattice speed, and is related to the speed of sound as $c_s = \frac{e}{\sqrt{3}}$.

The evolution of the distribution functions is described by the BGK collision terms:

$$f_i(\mathbf{x} + \mathbf{e}_i\Delta t, t + \Delta t) = f_i(\mathbf{x}, t) - \frac{f_i(\mathbf{x}, t) - f_i^{\mathrm{eq}}(\mathbf{x}, t)}{\tau} + K_i. \tag{4}$$

The equilibrium distribution function is defined as:

$$f_i^{\mathrm{eq}}(\rho(\mathbf{x}, t), \mathbf{u}(\mathbf{x}, \mathbf{t})) = w_i\rho(x)\left[1 + 3\frac{\mathbf{e}_i \cdot \mathbf{u}}{e^2} + \frac{9(\mathbf{e}_i \cdot \mathbf{u})^2}{2e^4} - \frac{3\mathbf{u}^2}{2e^2}\right], \tag{5}$$

where the weight coefficients for D2Q9 model are

$$w_i = \begin{cases} 4/9 & i = 0 \\ 1/9 & i = 1, \ldots, 4 \\ 1/36 & i = 5, \ldots, 8. \end{cases} \tag{6}$$

Table 1
Weights that yield the fourth, sixth and eighth order of isotropy interaction forces [13].

Order of isotropy	$\omega(1)$	$\omega(2)$	$\omega(3)$	$\omega(4)$	$\omega(5)$	$\omega(6)$	$\omega(8)$
4	1/3	1/12					
6	4/15	1/10		1/120			
8	4/21	4/45		1/60	2/315		1/5040

To incorporate a body force $\mathbf{F}$, an extra term K_i is included in the LBGK model. In this paper we use Guo's force term [17]:

$$\mathbf{K} = \left(1 - \frac{1}{2\tau}\right) w_i \left[3\frac{\mathbf{e}_i - \mathbf{u}}{e^2} + 9\frac{\mathbf{e}_i \cdot \mathbf{u}}{e^4}\mathbf{e}_i\right] \cdot \mathbf{F}, \tag{7}$$

and the Exact Difference Method (EDM) [14,18]:

$$K_i = f_i^{\mathrm{eq}}(\rho, \mathbf{u} + \Delta\mathbf{u}) - f_i^{\mathrm{eq}}(\rho, \mathbf{u}), \tag{8}$$

where the term $\mathbf{F}$ is the body force vector and $\Delta\mathbf{u} = \mathbf{F}\Delta t/\rho$. The macroscopic velocity $\mathbf{u}$ is computed as

$$\rho\mathbf{u}(\mathbf{x}, t) = \sum_i \mathbf{e}_i f_i(\mathbf{x}, t) + \frac{\Delta t\mathbf{F}}{2}. \tag{9}$$

Macroscopic transport equations for mass, momentum and energy can be derived from the Boltzmann equation using a Chapman–Enskog expansion [19]. The kinematic viscosity ν in the D2Q9 model is obtained as

$$\nu = c_s^2\left(\tau - \frac{1}{2}\right)\Delta t. \tag{10}$$

An interaction force term between the particles is used to describe the interparticle forces microscopically:

$$\mathbf{F}(\mathbf{x}, t) = -G\psi_\sigma(\mathbf{x}, t)\sum_{i=1}^{8}\omega(|\mathbf{e}_i|)\psi_{\bar\sigma}(\mathbf{x} + \mathbf{e}_i\Delta t, t)\mathbf{e}_i, \tag{11}$$

where σ and $\bar\sigma$ denote the different fluid components. G is a parameter determining the interaction strength $F(\mathbf{x}, t)$ between the neighbouring particles. It also determines whether the interaction is attractive or repulsive. To simulate a binary immiscible fluids system, the value of G should be kept positive so that a force will be generated to separate the fluids away from the interface. ψ_σ is the effective number density which is taken as component density: $\psi_\sigma = \rho_\sigma$ [11]. $\omega(|\mathbf{e}_i|)$ is a parameter related to the strength and order of isotropy of the interaction forces, as shown in Table 1.

To incorporate the interaction force, Shan and Chen proposed a force term scheme which only shifts the equilibrium velocity [12]. However, this force term scheme has been reported to be correct only if the relaxation time $\tau = 1$ [15,18]. This unfavourable feature can be eliminated using Guo's force term or the Exact Difference Method [17,20]. Both force terms have been incorporated in the Shan–Chen LB model and found to be independent of the equilibrium properties of τ; the difference between the Shan–Chen force term was shown to be on the order $O(F^2)$ [18,21,22]. To avoid the dependence of the equilibrium properties on the relaxation time, Guo's force term is used for the free energy and colour gradient models whereas the Exact Difference Method is used for the Shan–Chen model in this paper.

Shan [13] studied the spurious currents phenomenon of the Shan–Chen model. He concluded that the spurious currents are due to insufficient isotropy of the discrete gradient operator. For this reason, a new method of obtaining the discrete gradient operator with higher order isotropy was proposed. However, more adjacent nodes are needed to calculate the gradient operator. This will increase the amount of message exchanges required in parallel computing. Unfortunately, this method reduces the level of inherent parallelism of the lattice Boltzmann method. In this paper, we use a fourth and eighth order interaction force scheme [13] for the Shan–Chen multi-component model.

2.2. The free energy model

Swift et al. [9] developed a thermodynamically consistent binary fluid LB model by introducing an equilibrium state associated with a free energy functional, corresponding pressure tensors and chemical potentials. A correct choice of the collision rules ensures that the system evolves towards minimisation of the free energy functional.

The thermodynamic properties of a binary fluid system can be described by a Landau free energy functional

$$\Psi = \int_V \left(\psi_b + \frac{\kappa}{2}(\partial_\alpha\phi)^2\right)dv + \int_S \psi_s ds, \tag{12}$$

where ψ_b is the bulk free energy density and has the form

$$\psi_b = \frac{c^2}{3}\rho\ln\rho + \frac{A}{4}\phi^2(-2 + \phi^2). \tag{13}$$

A is a constant and was set as 0.04 in all simulations. ϕ is the order parameter representing the concentration of components, defined as

$$\phi = \frac{\rho_a - \rho_b}{\rho_a + \rho_b}. \tag{14}$$

The hydrodynamics and thermodynamics of the binary fluids are described by the Navier–Stokes equations and a convection–diffusion equation:

$$\frac{\partial \phi}{\partial t} + \nabla(\phi \mathbf{u}) = \mu \nabla^2 \phi, \tag{15}$$

where the parameter μ determines the diffusivity of the binary fluids system.

A new distribution function $g_i(x, t)$ is introduced to describe the concentration $\phi = \sum_i g_i$ and is related to the convection and diffusion. The distribution function $f_i(x, t)$ is related to the fluid density and momentum as usual.

The time evolution equation uses the Multiple Relaxation Time (MRT) scheme and can be described as:

$$\text{Collision Step: } f_i'(\mathbf{x}, t) = f_i(\mathbf{x}, t) - M^{-1} S M (f_i - f_i^{\text{eq}}), \tag{16}$$

$$g_i'(\mathbf{x}, t) = g_i^{\text{eq}}(\mathbf{x}, t). \tag{17}$$

$$\text{Streaming Step: } f_i(\mathbf{x} + \mathbf{e}_i \Delta t, t + \Delta t) = f_i'(\mathbf{x}, t), \tag{18}$$

$$g_i(\mathbf{x} + \mathbf{e}_i \Delta t, t + \Delta t) = g_i'(\mathbf{x}, t). \tag{19}$$

Using an appropriate choice of the equilibrium distribution functions, it is possible to reproduce the macroscopic equations in the continuum limit [9].

2.3. The colour gradient lattice Boltzmann model

An immiscible fluid model developed from Lattice Gas Cellular Automata was introduced by [5]. The particles in this model are coloured either red or blue and therefore it is normally called the colour gradient method. The surface tension is introduced by adding a perturbation to the collision operator while keeping the adherence to the Navier–Stokes equations in homogeneous regions. A recolouring step is invoked after the surface tension perturbation calculation in order to achieve zero diffusivity of one colour into the other. We use f_i^r, f_i^b and f_i to denote the distribution functions of the red fluid, the blue fluid and their combination respectively. A perturbation is computed to generate the surface tension. The surface tension can be expressed as a local anisotropy in the pressure: the pressure measured normal to the surface is larger than that tangential to the surface. The pressure in a LBM is proportional to the density, so the surface tension can be generated by preferentially placing particles in directions normal to the interface rather than tangential. Mass and momentum should be conserved. The colour gradient $\mathbf{C}$ is defined as:

$$\mathbf{C}(\mathbf{x}, t) = \sum_i \mathbf{e}_i \sum_j (f_j^r(\mathbf{x} + \mathbf{e}_i \Delta t, t) - f_j^b(\mathbf{x} + \mathbf{e}_i \Delta t, t)). \tag{20}$$

Perturbation of the populations gives

$$f_i''(\mathbf{x}, t) = f_i'(\mathbf{x}, t) + \sigma |\mathbf{C}(\mathbf{x}, t)| \left(\frac{(\mathbf{e}_i \cdot \mathbf{C})}{\mathbf{C} \cdot \mathbf{C}} - \frac{1}{2} \right), \tag{21}$$

where σ is a parameter to set the surface tension.

An alternative optimised perturbation term for the colour gradient LB model has been developed by Kehrwald [23] to improve the stability and accuracy. A further improvement based on the MRT collision scheme was proposed by Tölke et al. [24], reducing the spurious velocity, increasing the numerical stability and removing the dependency on viscosity. A redistribution of colour forces the particles to move towards the regions occupied by particles of the same colour. This recolouring step enables us to achieve separation of the fluids. It is carried out by the maximisation problem as given in Eq. (22), see [5]. Because the particles are forced to stay with the particles having the same colour, the colour gradient model is only able to simulate completely immiscible fluids.

$$W(f_i^{r''}, f_i^{b''}) = \max_{f_i^{r''}, f_i^{b''}} \left[\sum_i (f_{r_i}'' - f_{b_i}'') e_i \right]. \tag{22}$$

Subject to constraints:

$$\rho_r'' = \sum_i f_i^{r''} = \rho_r, \tag{23}$$

$$f_i^{r''} + f_i^{b''} = f_i. \tag{24}$$

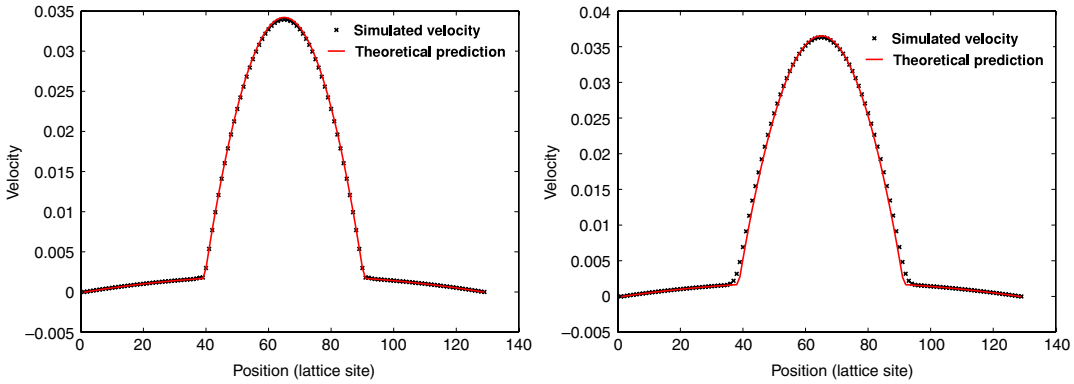

Fig. 1. Simulated velocity profiles for the colour gradient (left) and free energy model (right) with viscosity ratio 100.

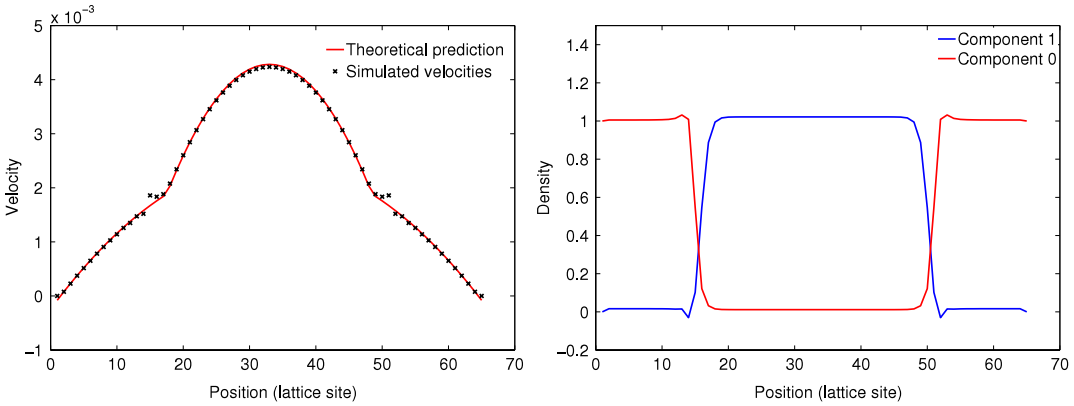

Fig. 2. Left: Simulated (black) and analytical (red) velocity profiles for Poiseuille flow of binary fluids with viscosity contrast for the Shan–Chen model; Right: Simulated density of the Shan–Chen model. The viscosity ratio between the two substances is 4. The initial densities are both set as 1. (For interpretation of the references to colour in this figure legend, the reader is referred to the web version of this article.)

A general colour gradient lattice Boltzmann model can be summarised as:

- Single phase collision using MRT scheme.
- Add a surface tension perturbation to f_i' obtaining f_i''.
- Recolouring.
- Streaming.

In both the free energy model and the colour gradient model, only the value of distribution functions of the nearest neighbour nodes are needed, which keeps the inherent parallelism of the lattice-Boltzmann method.

3. Comparison study

We use three multi-component LB models for two problems: Poiseuille flow for binary fluids with viscosity contrast and capillary fingering. The numerical results are presented and compared with theoretical predictions. The thickness of the interface, limitations of the models and numerical stability are also discussed. A summary is given to show the capability and limitation of every model.

3.1. Poiseuille flow simulation for a binary immiscible fluid system with viscosity contrast

We carry out simulations of two fluids with a kinematic viscosity contrast in a channel and compare with theoretical predictions in Fig. 1. The domain is periodic in y direction and bounded with non-slip walls. The system is initialised with substance 0 in the middle and substance 1 on both sides near the walls. An initial density value of 1 is applied to both substances 0 and 1. The force acceleration applied to each substance is 10^{-6}.

Fig. 2 shows the velocity and density profile for the Shan–Chen model with viscosity ratio 4. The interactions were calculated using an eighth order isotropy scheme and the Exact Difference Method was employed to incorporate the interaction forces between the components. The simulation results are generally in good agreement with the analytical

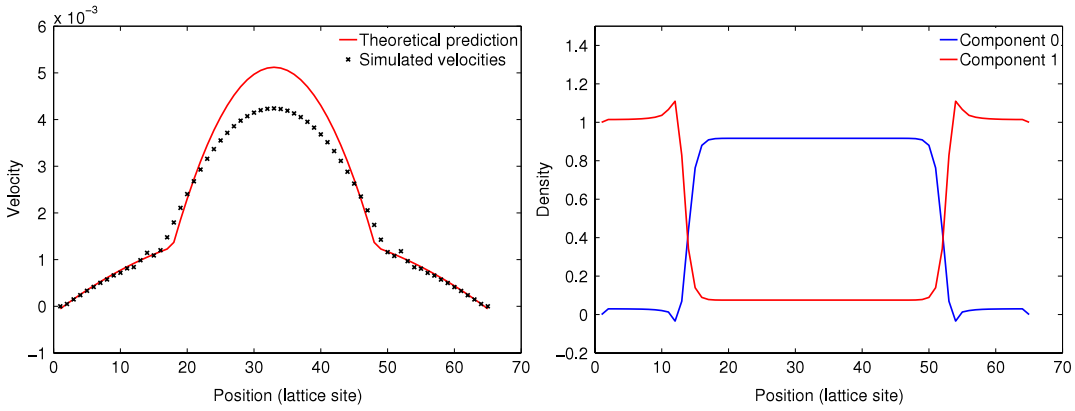

Fig. 3. Simulated velocity (left) and density (right) profiles for the Shan–Chen model. The viscosity ratio between the two substances is 10. The initial densities are both set as 1.

solution [25], away from the interfaces. The density profile shows that the two components are immiscible except for some noise near the interfaces. It is worth mentioning that a very strong interaction is required to achieve an immiscible interface; we observed very high spurious velocities up to 10^{-1} (in lattice units) near the interfaces. Fig. 3 shows the velocity profile for the Shan–Chen model with viscosity ratio 10. We observe that the simulation result does not match the analytical solution and some noise is found near the interface. This phenomenon has also been found by Sukop et al. [26]. To explore the reason for the poor agreement with the theoretical prediction, the density profile of the two substances is shown as well. In the density profile, we observe significant diffusion between the two substances. The concentration of substance 0 decreases in the middle and increases in the domains near the walls. To separate the two components, a stronger interaction is needed. However, in that case the simulation becomes unstable due to high spurious velocities caused by the strong interactions. A previous study showed good agreement with theoretical predictions for fluids having a viscosity ratio less than 6 [25]. It turns out to be difficult to calculate the flow of binary fluids with a viscosity ratio larger than 6 as numerical instabilities emerge. We observe that the thickness of the interface is significant (around 10 lattice sites). The deviation from the analytical solution is probably due to the low resolution of the channel as some very good results using fine resolution have been reported [14,18]. However, this will increase the computational cost of problem. In summary, we believe that the use of the Shan–Chen model, with regard to simulation of flow in real porous media geometries, is limited for the following reasons:

- The wide liquid–liquid interface is unfavourable for the simulation of flow in porous media, particularly reservoir rocks, where the average pore radius is typically around 10–30 (l.u.).
- It is difficult to increase the resolution of pore space images obtained from X-ray micro tomography (XMT) due to experimental limitations.
- Even if it is possible to increase the resolution, this would substantially increase the computational burden.

For comparison, we have carried out the same calculations using Guo's force term. We observe that the agreement with the analytical solution is not as good as for the Exact Difference Method (EDM). Also the spurious velocities observed near the interfaces are more significant for the Guo model compared to EDM.

The simulation results of both the free energy model and the colour gradient model give excellent agreement with the analytical solution. The concentration profile is also as expected. Two immiscible fluids are constrained in their respective areas and no unexpected diffusion is discovered. We note that the interface thickness of the free energy model is around 6 lattice units (l.u.) and the interface location is found at $x = 38$ instead of their initial position of $x = 35$, so that an interfacial movement of 3 lattice units is discovered from the result. The reason for this interface shifting is not clear and needs further investigation. The interface thickness of the colour gradient model is around 4 l.u., which is smaller than that of the free energy model. An interfacial shift is observed in the colour gradient model of around 1.5 l.u., which is significantly smaller than the free energy model. The recolouring algorithm separates the two immiscible fluids very well and gives nearly 0 diffusivity as expected.

The thickness of the interface for different multi-component models varies. The thicknesses of the interfaces are studied in the Poiseuille flow simulations with a viscosity ratio of 10 and a surface tension of 0.005. The Shan–Chen model generates a thickness of 6 l.u., while the free energy model and the colour gradient model give 4 and 2–3 lattice units respectively.

3.2. Capillary fingering simulation

Capillary fingering is a well-known hydrodynamic instability which occurs in various displacements during oil/gas production. Here we consider one fluid which is displaced by a second one, having a different viscosity, along a channel

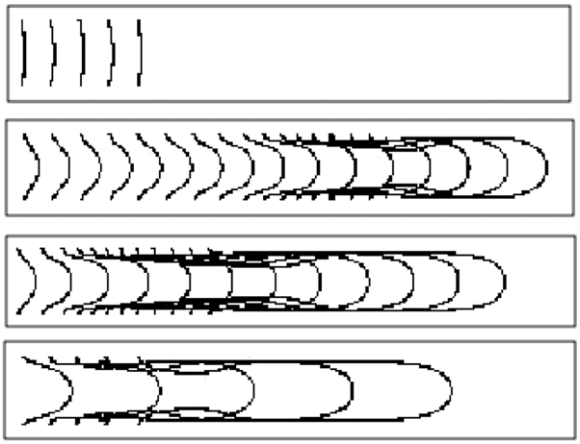

Fig. 4. From top to bottom: Fingering evolution for the free energy model with surface tensions of 0.06780, 0.03890, 0.01985, 0.00992 at a time interval of 1000 time steps. Viscosity ratio is 10; the tip velocity is 0.01. The number of snapshot were different due to the different time required for the evolution of fingers. For large surface tension, the fingers develop very slowly. For low surface tension, on the other hand, we find very long fingers (developing very quickly).

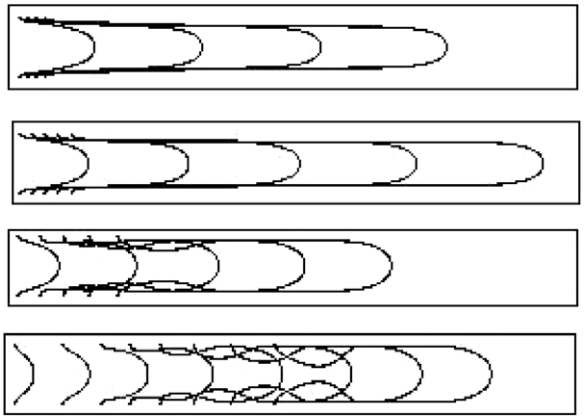

Fig. 5. From top to bottom: Fingering evolution for the colour gradient model with surface tensions of 0.03890, 0.01985, 0.00992, 0.00496 at a time interval of 1000 time steps. Viscosity ratio is 20; the tip velocity is 0.05.

with non-slip walls. A growing finger of the driving fluid will be produced if the Capillary number Ca is big enough.

$$\mathrm{Ca} = \frac{u_t \rho \nu_2}{\sigma}, \tag{25}$$

where u_t is the velocity of the tip of the finger and ν_2 is the viscosity of driving fluid. σ is the surface tension.

Chin et al. studied viscous fingering using the Shan–Chen model [25]. Although fingering structures were observed in their simulations, the development of a finger is clearer in simulations at higher surface tensions, which is counterintuitive. We normally expect that increased surface tension is not favourable to the generation of fingers. It is not clear whether these structures were produced due to viscous fingering or due to other effects [25]. Numerical instability and high diffusivity were also found in the simulation when the viscosity ratio is larger than 7.

Here we use the colour gradient model and the free energy model to study viscous fingering. A domain with grid size 512×32 is used in the simulation. The first half of the domain contains substance 0 and the rest is occupied by phase 1. Periodic boundary conditions are used in x direction and bounded with non-slip boundaries. A pressure gradient is imposed by applying a body force in the x direction. Fig. 4 shows the evolution of fingers for binary fluids with a viscosity ratio of 20 and a tip velocity of 0.01, simulated by the free energy model. From top to bottom, these are finger evolutions for surface tension values of 0.06780, 0.03890, 0.01985 and 0.00992 respectively. No finger will be produced if the surface tension is high. When the surface tension decreases, fingers are observed. However, with decreasing surface tension, less stable interfaces are produced. Fig. 5 shows the evolution of the fingers of the same binary fluids with a larger tip velocity of 0.05, calculated by the colour gradient model. In all cases, stable fingers are observed. Halpern et al. [27] studied the fingering phenomenon in a channel, by measuring the width of the fingers as a function of the Capillary number Ca. We show our results obtained from the free energy and colour gradient models in comparison with the results from [27] in Fig. 6.

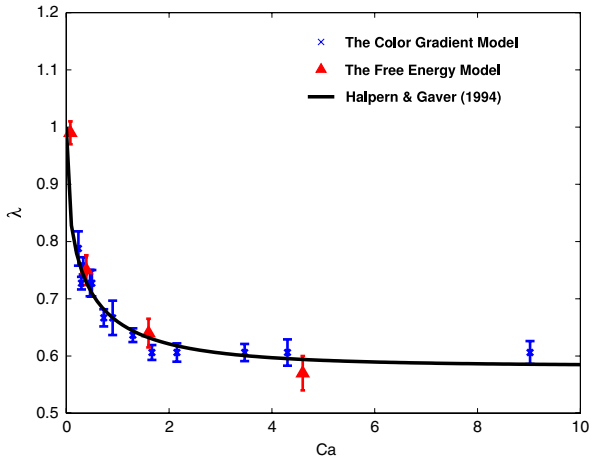

Fig. 6. Finger width as a function of Capillary number. Our simulation results from the free energy and colour gradient model model are shown as triangles and stars respectively, in comparison with the results from Halpern shown as a solid black line.

Table 2
Quantitative comparison of three multi-component LB models.

	The Shan–Chen pseudo potential model	The free energy model	The colour gradient model
Maximum density ratio	Up to 10^9 [14]	1	1
Maximum viscosity ratio	5	120 (static interfaces) 20 (dynamic interfaces)	120 (static interfaces) 20 (dynamic interfaces)
Interface thickness (Poiseuille flow simulation)	10 l.u.	5 l.u.	2–3 l.u.
Interface shifting distance (Poiseuille flow)	10 l.u.	5 l.u.	2–3 l.u.
Ability of simulating capillary fingering	No	Yes	Yes
Inherent parallelism	Low	High	High
Diffusion	High diffusivity interface	Diffusivity can be controlled by a single parameter	Complete immiscible, no diffusion on the surface

Good agreement is achieved although some small discrepancies are found. These discrepancies might have arisen from the boundary conditions. The free energy model gives better agreement for low Capillary number simulations and the colour gradient models did better in high Capillary number simulations. These numerical examples show that fingering phenomena can be captured properly by both the free energy model and the colour gradient model. It is worth mentioning that the numerical stability for both the free energy model and the colour gradient model is similar. The maximum viscosity ratio for dynamic interface simulations is around 20. To achieve a higher viscosity ratio, an optimised perturbation term based on MRT collision scheme needs to be used. In this case, the viscosity ratio can be increased to 1000 with reasonable numerical stability [24].

4. Summary

The advantages and limitations of the Shan–Chen model, the colour gradient model and the free energy model have been investigated and directly compared with regard to seven different aspects:

1. the maximum density ratio of binary fluids that can be achieved;
2. the maximum viscosity ratio of binary fluids that can be achieved;
3. interfacial thickness in Poiseuille flow;
4. interface shifting distance in Poiseuille flow;
5. level of inherent parallelism;
6. ability to describe capillary fingering;
7. diffusion properties.

It has been observed that the Shan–Chen model is capable of simulating high density ratio fluids [18,28]. As such, it is a promising tool for liquid–gas systems, but gives relatively low numerical stability and wide interfaces for multi-component immiscible systems. For this reason, this model may not be the optimal solution for simulation of immiscible flows [29]. Both the colour gradient and Oxford free energy model are capable of simulating fluids with significant viscosity contrast, and recover the analytical solutions of Poiseuille flow and fingering simulations. In our study, we found that the maximum viscosity ratio of these two models depends on the type of problem. If the interface is static, fluids with a viscosity ratio up to 120 can be simulated. However, for dynamic interface simulations, this value decreases to 20. A full quantitative comparison of the three multi-component LB models considered is presented in Table 2. We conclude that the Oxford free

energy and colour gradient models seem appropriate to simulate the flow of binary fluids with high viscosity contrast and high numerical stability. This is of great importance for the study of immiscible flow in porous media, in particular for CO_2 storage and Enhanced Oil Recovery (EOR) operations.

Acknowledgements

This work was carried out as part of the activities of the Qatar Carbonates & Carbon Storage Research Centre (QCCSRC) at Imperial College London. We gratefully acknowledge the funding of QCCSRC provided jointly by Qatar Petroleum, Shell, and the Qatar Science and Technology Park, and their permission to publish this research.

References

[1] Z. Guo, C. Zheng, Theory and Applications of Lattice Boltzmann Method, Science Press, Beijing, 2008.
[2] E.S. Boek, M. Venturoli, Lattice–Boltzmann studies of fluid flow in porous media with realistic rock geometries, Comput. Math. Appl. 59 (7) (2010) 2305–2314.
[3] G. Doolen, Lattice Gas Methods for Partial Differential Equations: A Volume of Lattice Gas Reprints and Articles, Including Selected Papers from the Workshop on Large Nonlinear Systems, Held August, 1987 in Los Alamos, New Mexico, in: Santa Fe Institute Studies in the Sciences of Complexity, Addison-Wesley, 1990.
[4] S. Chen, Z. Wang, X. Shan, G.D. Doolen, Lattice Boltzmann computational fluid dynamics in three dimensions, J. Stat. Phys. 68 (3–4) (1992) 379–400.
[5] A.K. Gunstensen, D.H. Rothman, S. Zaleski, G. Zanetti, Lattice Boltzmann model of immiscible fluids, Phys. Rev. A 43 (8) (1991) 4320–4327.
[6] D. Grunau, S. Chen, K. Eggert, A lattice Boltzmann model for multiphase fluid flows, Phys. Fluids A 5 (10) (1993) 2557–2562.
[7] J. Tölke, M. Krafczyk, M. Schulz, E. Rank, Lattice Boltzmann simulations of binary fluid flow through porous media, Philos. Trans. R. Soc. Lond. A Math. Phys. Eng. Sci. 360 (2002) 535.
[8] U. D'Ortona, D. Salin, M. Cieplak, R.B. Rybka, J.R. Banavar, Two-color nonlinear Boltzmann cellular automata: surface tension and wetting, Phys. Rev. E 51 (4) (1995) 3718–3728.
[9] M.R. Swift, E. Orlandini, W.R. Osborn, J.M. Yeomans, Lattice Boltzmann simulations of liquid–gas and binary fluid systems, Phys. Rev. E 54 (5) (1996) 5041–5052.
[10] C.M. Pooley, K. Furtado, Eliminating spurious velocities in the free-energy lattice Boltzmann method, Phys. Rev. E 77 (4) (2008) 046702.
[11] X. Shan, H. Chen, Lattice Boltzmann model for simulating flows with multiple phases and components, Phys. Rev. E 47 (3) (1993) 1815–1819.
[12] X. Shan, G. Doolen, Multicomponent lattice-Boltzmann model with interparticle interaction, J. Stat. Phys. 81 (1) (1995) 379–393.
[13] X. Shan, Analysis and reduction of the spurious current in a class of multiphase lattice Boltzmann models, Phys. Rev. E 73 (4) (2006) 047701.
[14] A.L. Kupershtokh, D.A. Medvedev, D.I. Karpov, On equations of state in a lattice Boltzmann method, Comput. Math. Appl. 58 (5) (2009) 965–974.
[15] A.L. Kupershtokh, D.I. Karpov, D.A. Medvedev, C.P. Stamatelatos, V.P. Charalambakos, E.C. Pyrgioti, D.P. Agoris, Stochastic models of partial discharge activity in solid and liquid dielectrics, IET Sci. Meas. Technol. 1 (6) (2007) 303–311.
[16] Y.H. Qian, D. d'Humières, P. Lallemand, Lattice BGK models for Navier–Stokes equation, Europhys. Lett. 17 (6) (1992) 479–484.
[17] Z. Guo, C. Zheng, B. Shi, Discrete lattice effects on the forcing term in the lattice Boltzmann method, Phys. Rev. E 65 (4) (2002) 046308.
[18] A.L. Kupershtokh, New method of incorporating a body force term into the lattice Boltzmann equation, in: Proc. 5th International EHD Workshop, University of Poitiers, Poitiers, France, 2004, pp. 241–246.
[19] D.A. Wolf-Gladrow, Lattice-Gas Cellular Automata and Lattice Boltzmann Models, in: Lecture Notes in Mathematics, Springer, 2000.
[20] H. Huang, M. Krafczyk, X. Lu, Forcing term in single-phase and Shan–Chen-type multiphase lattice Boltzmann models, Phys. Rev. E 84 (4) (2011) 046710.
[21] Z. Yu, L.S. Fan, An interaction potential based lattice Boltzmann method with adaptive mesh refinement (AMR) for two-phase flow simulation, J. Comput. Phys. 228 (17) (2009) 6456–6478.
[22] Z. Yu, A novel lattice Boltzmann method for direct numerical simulation of multiphase flows, Ph.D. Thesis, The Ohio State University, 2009.
[23] D. Kehrwald, Numerical analysis of immiscible lattice BGK, Ph.D. Thesis, Dissertation, Fachbereich Mathematik, Universität Kaiserslautern, 2002.
[24] J. Tölke, S. Freudiger, M. Krafczyk, An adaptive scheme using hierarchical grids for lattice Boltzmann multi-phase flow simulations, Comput. Fluids 35 (8) (2006) 820–830.
[25] J. Chin, E.S. Boek, P.V. Coveney, Lattice Boltzmann simulation of the flow of binary immiscible fluids with different viscosities using the Shan–Chen microscopic interaction model, Philos. Trans. R. Soc. Lond. A Math. Phys. Eng. Sci. (2002) 547–558.
[26] M.C. Sukop, D.T. Thorne, Lattice Boltzmann Modeling: An Introduction for Geoscientists and Engineers, Springer Verlag, 2007.
[27] D. Halpern, D.P. Gaver, Boundary element analysis of the time-dependent motion of a semi-infinite bubble in a channel, J. Comput. Phys. 115 (2) (1994) 366–375.
[28] P. Yuan, L. Schaefer, Equations of state in a lattice Boltzmann model, Phys. Fluids 18 (2006) 042101.
[29] X. Shan, Simulation of Rayleigh–Bénard convection using a lattice Boltzmann method, Phys. Rev. E 55 (3) (1997) 2780–2788.